

# Outcome of Copper Incorporation in the Photocatalytic Activity of Cadmium Oxide Nanoparticles

D. J. Jeejamol<sup>1</sup>, K. Jayakumari<sup>2</sup>, A. Moses Ezhil Raj<sup>1\*</sup>

<sup>1</sup>*Department of Physics & Research Centre, Scott Christian College (Autonomous),  
Nagercoil – 629 003, India*

<sup>2</sup>*Department of Physics, Sree Ayyappa College for Women, Chunkankadai, India*

**Abstract:** Cadmium oxide (CdO) nanoparticles doped with different wt. % of copper have been prepared by means of chemically controlled co-precipitation method. The powder X-ray diffraction patterns of the prepared samples revealed the formation of single phase polycrystalline face centered cubic (Fm  $\bar{3}$  m) CdO structure even after doping with Cu<sup>2+</sup>. Initially the crystallinity of CdO was improved on Cu doping, however, with the increase of dopant concentration, a change in lattice constant was noticed. Amorphization and/or composite formation were not observed for the present level of doping. The metal oxide phase formation was again established from its Cd-O stretching band at about 460 cm<sup>-1</sup> and by the broad band with poor resolved shoulders at about 580 and 1000 cm<sup>-1</sup> in the infrared spectra. Inclusion of Cu<sup>2+</sup> in the CdO lattice was further ascertained from slight shift in peak positions and changes in its width. Raman spectral bands in pure and intentionally doped CdO around 70 and 260 cm<sup>-1</sup> can be attributed to the LA-TA or LO-TO and TA+TO modes at the L-point of Brillouin zone respectively. The shift in the prominent bands and change in the Raman profile evidently proved the replacement of Cu<sup>2+</sup> in the place of Cd<sup>2+</sup>. The photocatalytic activity of pure and doped CdO were tested for the degradation of methylene blue (MB) in aqueous medium under visible light. Copper doped CdO exhibited substantially higher visible-light-driven photocatalytic activity and the percentage of color abatement in the aqueous solution for 5 hours was good for the samples calcined at 400°C (71% for pure CdO, 79% for 1% Cu doped CdO and 72% for 2% Cu doped CdO). The degradation rate of methylene blue followed the pseudo-first order kinetics and the rate constant obtained (0.3 to 0.7 hr<sup>-1</sup>), proved the pure and Cu doped CdO nanoparticles as the best photo catalyst for the removal of color from textile waste water.

**Keywords -** FT-IR, FT-Raman, Nanoparticles, Photocatalytic, XRD

---

\*Corresponding author

e-mail: ezhilmoses@yahoo.co.in (A. Moses Ezhil Raj) | Phone: +91 4652 232888 | Fax: +91 4652 229800

## I Introduction

Transparent conducting oxides (TCO) have attracted growing attention over the last decades as significant components of technological applications. Among these oxide, CdO is an important TCO with a variety of optoelectronic applications like, solar cells, optical communications, flat panel display [1–3]. CdO is an n-type semiconductor with optical band gap of ~2.5 eV [4]. The n-type conduction of undoped CdO is attributed to its native oxygen vacancies and cadmium interstitials. Therefore, the conductivity of CdO nanoparticles can be controlled by those native defects [5] or by doping with metallic ions like: In [6], Sn [5], Al [7], Sc [8], and Y [9]. Generally, it was observed that doping with ions of radius less (to a limited extend) than that of Cd<sup>2+</sup> slightly shrinks the CdO lattice parameters, increases the apparent energy gap, increases the carrier mobility and concentration, and hence increases the conductivity. For solar cell and other optoelectronic applications, it is welcomed to dope CdO with some ions in order to increase both the conductivity as well as the transmittance.

Published by SLGP. Selection and/or peer-review under responsibility of ICISEM 2016. Open access under CC BY-NC-ND license.

Due to the unique optical and electrical properties of CdO, it has a wide range of applications such as phototransistors, solar cells, catalyst, chemical sensors, electroplating baths, liquid crystal displays, IR detectors, transparent electrodes and gas sensors [10, 11]. Most of the semiconducting oxides are photocatalysts. Among the metal oxide semiconductors, cadmium oxide is found to be a promising candidate for this application, as it can be activated with visible light ( $<590$  nm). Different soft chemical methods such as co-precipitation, sol-gel and hydrothermal synthesis have been attempted to obtain pure CdO and doped CdO nanoparticles [12]. Here in the preparation of cadmium oxide nanoparticles via chemically controlled co-precipitation method followed by calcination and its usefulness as photocatalyst to degrade methylene blue, which is a basic aniline dye,  $C_{16}H_{18}N_3S$  utilized in coloring paper, temporary hair coloring, dyeing cotton and wools, and coloring of paper stocks has been investigated. Structural characterization of pure and  $Cu^{2+}$  doped CdO nanoparticles were done to test their appropriateness as photocatalysts.

## II Experimental

In the co-precipitation method, ammonium hydroxide was added drop-wise to 0.5M cadmium acetate dihydrate ( $Cd(CH_3COO)_2 \cdot 2H_2O$ ) under constant stirring until the pH value of the solution attains 8. Resulted precipitate was then filtered and washed repeatedly after 18 to 20 hours using double distilled water to remove impurities. The hydroxide thus formed was calcined at different temperatures 400, 600 and 800°C for 2h to produce nanocrystalline powders. For doped samples the Cu source, 0.5M copper chloride was dissolved in required amounts along with the 0.5M cadmium acetate. Structural information was obtained from the x-ray diffraction patterns recorded in PANalytical X'pert-pro instrumentation. Fourier transform infrared (FT-IR) spectra were recorded with a Thermo Nicolet, Avatar 370 spectrometer in the range 400-4000  $cm^{-1}$  using KBr pellet technique. Raman spectra were recorded with a BRUKER RFS 27: Stand alone FT-Raman Spectrometer. To investigate the photocatalytic property, 162 mg of the photocatalysts was dispersed in the 50 ml methylene blue aqueous solution with an initial concentration of  $10^{-5}$  mol/L. The photodegradation of methylene blue ( $C_{16}H_{18}N_3S$ ) was then studied from the change in optical property of methylene blue (MB) aqueous solution in presence of pure and Cu doped CdO nanoparticles before exposure of light and after exposure of light for 1h difference using the Varian Cary-5000 UV spectrophotometer.

## III Results and discussion

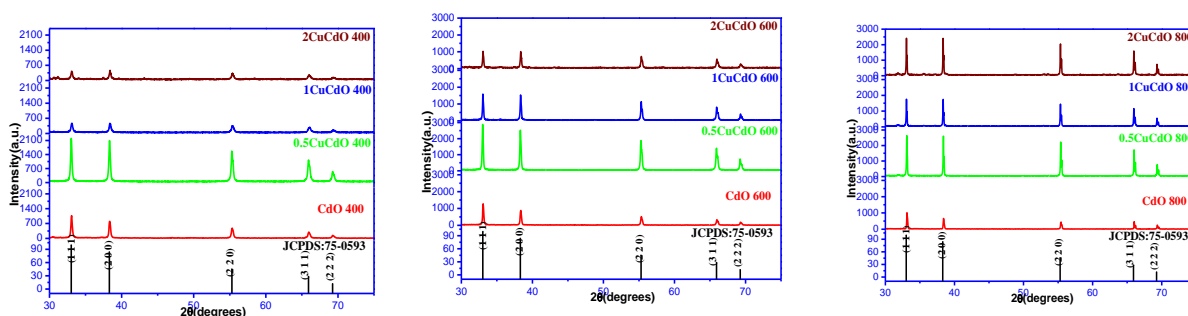


Fig. 1 XRD patterns of pure and Cu doped CdO nanoparticles calcined at 400°C, 600°C and 800°C

In the XRD patterns of pure and  $Cu^{2+}$  doped CdO nanoparticles (Fig. 1), the observed “ $d$ ” spacings and the respective prominent peaks correspond to reflections of (111), (200), (220), (311) and (222) planes and are in good agreement with the standard data (JCPDS card no.: 75-0593). Peak positions of the crystallized pure and doped CdO thus corresponds to the face centered cubic structure. To some extent the volume of unit cell of host CdO crystalline structure decreased with Cu doping due to smaller size of  $Cu^{2+}$  dopant ions in contrast to that of  $Cd^{2+}$ . The lodging of  $Cu^{2+}$  in the position of  $Cd^{2+}$  leads to the shrinkage of lattice constants after doping. However, the substitution of copper does not affect the structure of CdO. [13]. The decrease of intensity of the reflections with the increase of Cu% doping level, results in the deterioration of crystal structure of CdO. Compression in the unit cell on doping was evidenced from the slight shift in diffraction peaks in the range 0.016–0.115° towards higher angles in  $Cu^{2+}$  doped CdO nanopowder [14]. This may be due to a small variation in the particles size [15]. The variations in the structural parameters with dopants and with calcination temperature are listed in Table 1.

**Table 1 Variation in lattice parameter, volume and crystallite size**

Sample Details	Lattice Parameter (a) Å	Volume Å <sup>3</sup>	Scherrer Formula D (nm)
CdO 400	4.6937	103.40	39.32
CdO 600	4.6925	103.33	60.09
CdO 800	4.6852	102.84	107.25
0.5CuCdO 400	4.6978	103.67	73.83
0.5CuCdO 600	4.6984	103.71	85.03
0.5CuCdO 800	4.6878	103.01	139.88
1CuCdO 400	4.6908	103.22	46.57
1CuCdO 600	4.6952	103.5	93.99
1CuCdO 800	4.6921	103.3	138.32
2CuCdO 400	4.6929	103.35	47.96
2CuCdO 600	4.6936	103.4	74.17
2CuCdO 800	4.6914	103.26	110.69

The FTIR spectra (Fig. 2) of undoped and Cu<sup>2+</sup> doped CdO nanopowder exhibited various vibrational bands related to metal oxides. The bands observed at 645–728 cm<sup>-1</sup> are assigned to Cd-O metal oxide bonding [16]. CdO phase formation was further confirmed from its Cd-O stretching band at about 460 cm<sup>-1</sup> and by the broad IR band with poor resolved shoulders at about 580 and 1000 cm<sup>-1</sup> in the FTIR spectra [17]. Incorporation of Cu in the CdO lattice was ascertained from the slight shift in vibrational band positions as well as from the additional band, obtained on doping, around 550cm<sup>-1</sup> which was due to Cu-O stretching.

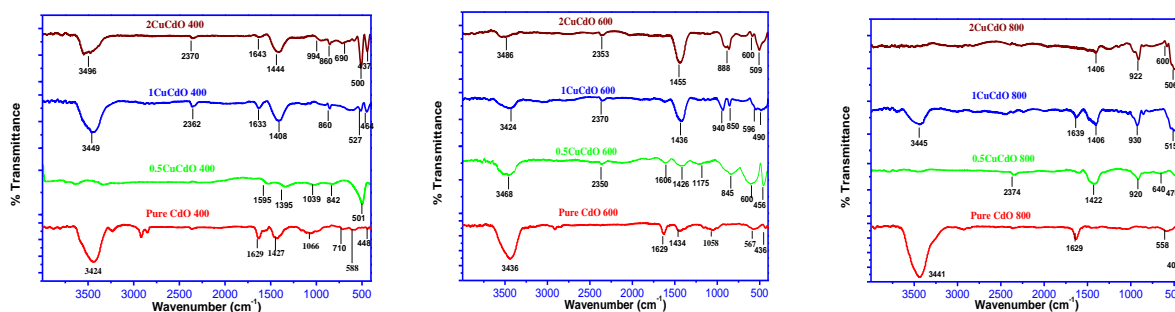


**Fig. 2 FTIR Spectra of pure and Cu doped CdO nanoparticles**

The deconvoluted (Gaussian multiple peak fit) Raman scattering (RS) peaks for pure and Cu doped CdO shown in Fig. 3 can be attributed to its weak second-order RS processes [18]. In the 50–80 cm<sup>-1</sup> range the difference, two-phonon density of states exhibits a maximum which can be attributed to LA-TA or LO- TO difference modes. In the 90–120 cm<sup>-1</sup> region the one-phonon density of states exhibits sharp features arising from TA modes. The distinct peak at ~260 cm<sup>-1</sup> was identified as a TA + TO mode at the L-point of Brillouin zone (BZ) according to two-phonon density of states (PDOS) calculations [19]. The absorption bands in the region 200–300 cm<sup>-1</sup> correspond to Cd–O vibrational modes [20].

The observed shift in the wave number values of the different modes and the broad nature of the Raman bands indicate that the doping of CdO produces stress in CdO nanoparticles which is in support of the XRD findings. According to the molecular theory of vibration, Raman modes are specifically sensitive to local geometric disorientation to the neighboring disorder especially from sub-lattices or electric defects resulting from substitutions or vacancies. This point to the fact that the broadening of the characteristic Raman modes of crystalline CdO may originate from both the local disorientation and neighboring disorder introduced by Cu incorporation to the CdO host lattice [21]. Profile of the Raman peaks depends on the crystallization, residual stress, structural disorder and crystal defect in a sample and as a result the profile of the Raman peaks changed on doping and on different calcinations temperatures. The additional bands in the doped samples that correspond to the silent modes of CdO arise from the breakdown of the translational crystal symmetry induced by the non-native ions and defects that can result in the change of Raman activation and Raman peak shift.

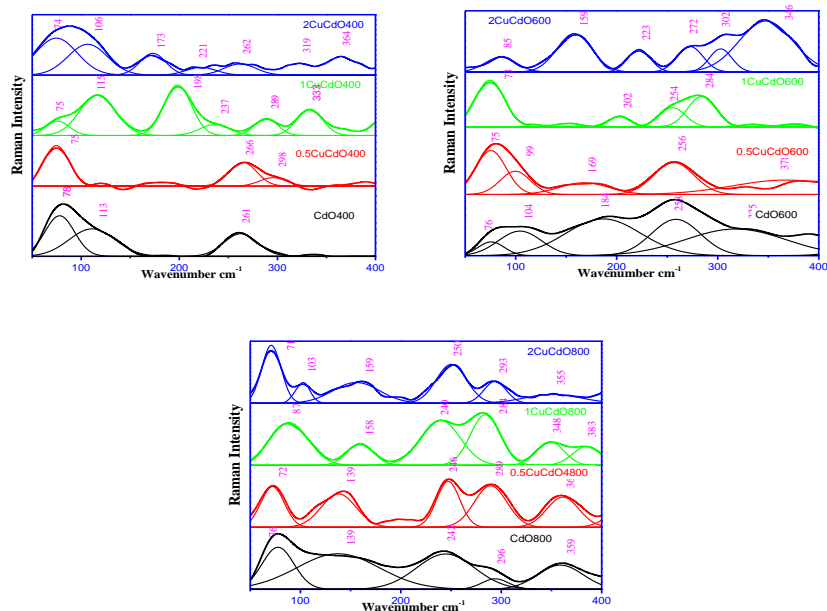


**Fig. 3 FT-Raman Spectra of pure and Cu doped CdO nanoparticles for different calcination temperatures**

In nature, semiconductors displays high absorbing behaviors based on their band-gap energy. The exceptional nanostructure of doped morphology allows them to absorb the solar-lights and promote photocatalysis with higher efficiency [22, 23]. Considering the solar-light absorption of the nanostructures, it is intended simulated block-structures to act as photo-catalysts as well as solid phase adsorbent with higher capacity and sensitivity. In the present study, the prospect of using pure and Cu doped CdO semiconductor nanomaterial for the photocatalytic degradation of methylene blue dye (MB) was explored in the presence of visible irradiation. Solution with  $10^{-5}$  M dye and 0.025 M photocatalyst was magnetically stirred for 5h period under sunlight. Decolorizing or removal efficiencies were calculated based on the absorption intensity of the methylene blue (MB) solutions at different times [24]. The optical absorption peak of MB at 665 nm was chosen to monitor the photocatalytic degradation process. With time increasing from 0 to 1 hr, the intensity of the characteristic absorption band at 665 nm decreased gradually, suggesting that the methylene blue was gradually photodegraded by the pure and doped CdO photocatalysts (Fig. 4). Starting from these absorption spectra, the dye concentration '[MB]' at a given time 't', normalized as a function of time (h) is shown in Fig. 5 As can be seen, the '[MB]' vs. time has an exponential decay, characteristic of a first order reaction:  $[MB] = [MB]_0 e^{-kt}$ , where, 'k' is the rate constant and '[MB]<sub>0</sub>' is the initial MB concentration. The linear fit between  $\ln([MB]_0/[MB])$  and irradiation time can be approximated as pseudo-first-order kinetics [25] (Fig. 6), the slope of which gives the rate constant 'k'. 'k' value was found to be in the range  $0.29755$  to  $0.73861 \text{ hr}^{-1}$ , which proves the best photocatalytic activity of pure and Cu doped CdO nanoparticles that make it a viable alternative for the removal of color from textile waste water.

The outcome of kinetic analyses show that a decrease in the MB concentration results in an increase in the apparent photocatalytic activity of the CdO nanoparticles. The entire photocatalysis process depends on the properties of the catalyst, and the effective light intensity in the system. Small-sized nanoparticles with great surface area are proficient substrates for absorption of light [26] which is essential for the enhancement of photocatalytic activity. Accordingly, the percentage of degradation of methylene blue in the aqueous solution for 5 hours is good for the samples calcined at low temperature (400°C): 71% for pure CdO (Crystallite size = 39 nm), 79% for 1% Cu doped CdO (Crystallite size = 46 nm) and 72% for 2% Cu doped CdO (Crystallite size = 48 nm).

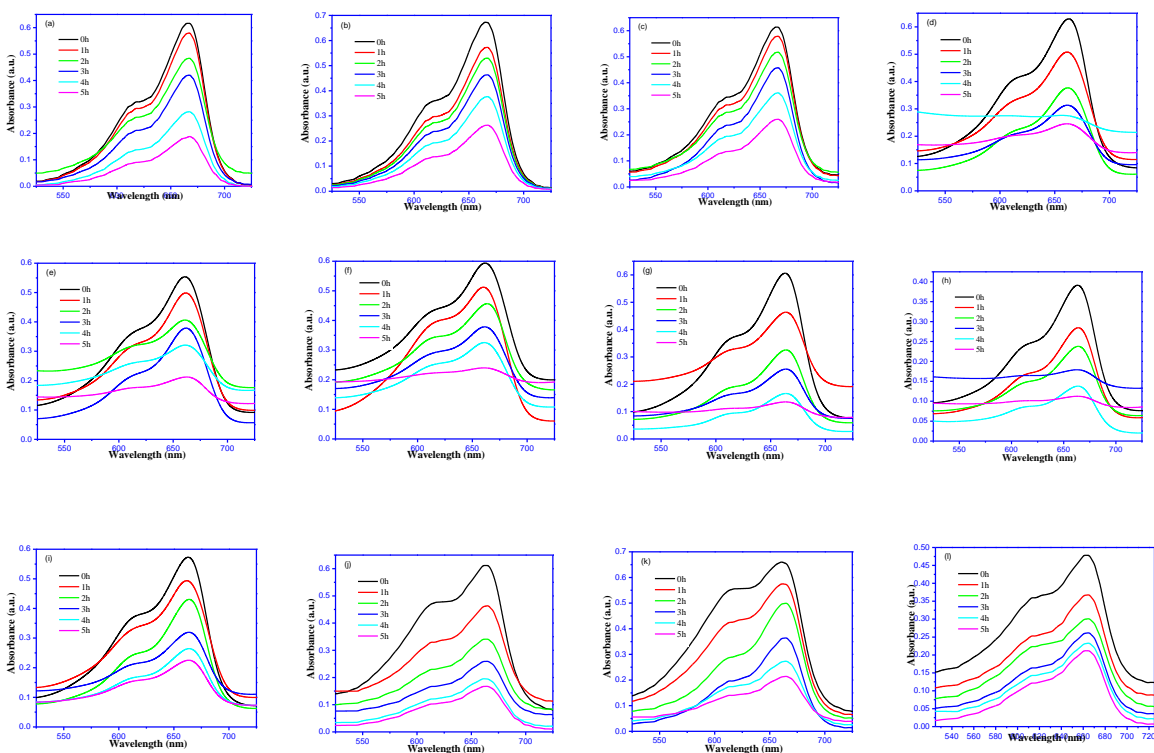


**Fig. 4** Variation of intensity of the absorption bands with irradiation time (a) CdO400 (b) CdO600 (c) CdO800 (d) 0.5CuCdO400 (e) 0.5CuCdO600 (f) 0.5CuCdO800 (g) 1CuCdO400 (h) 1CuCdO600 (i) 1CuCdO800 (j) 2CuCdO400 (k) 2CuCdO600 (l) 2CuCdO800

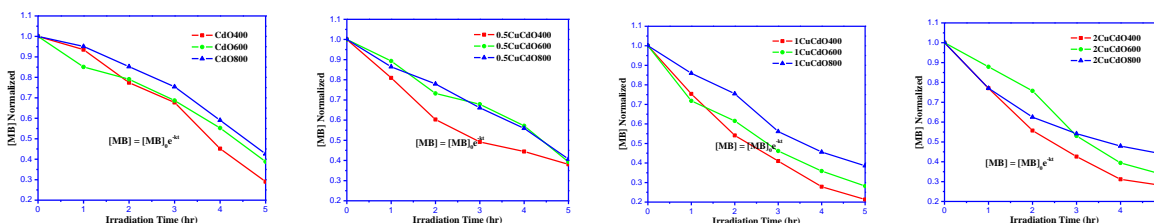


**Fig. 5** The dye concentration '[MB]' at a given time 't' normalized as a function of time

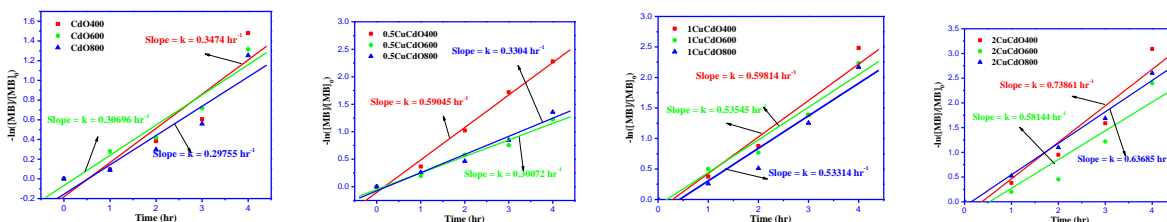


Fig. 6 The linear fit between  $\ln([MB]_0/[MB])$  and irradiation time

## IV Conclusion

The present study outlines synthesis of pure and  $\text{Cu}^{2+}$  doped cadmium oxide nanopowder using the chemical co-precipitation method followed by calcination. XRD patterns revealed cubic (fcc) structure for the prepared pure and  $\text{Cu}^{2+}$  doped CdO nanoparticles. The values of lattice parameter, unit cell volume and crystallite size are calculated based on the XRD data. There were some changes in the crystallite size of pure CdO with the addition of Cu-dopant. Accordingly, it is possible to control the nanostructure shape and size by the proper doping of parent. By FTIR spectroscopy, the functional groups present in the pure and  $\text{Cu}^{2+}$  doped CdO nanopowder were examined and the doping was confirmed by the band appeared around  $550\text{cm}^{-1}$  which was due to the Cu-O stretching. In the photocatalytic activity, the color abatement was maximal for the pure and doped samples calcined at  $400^\circ\text{C}$ . Thus, it can be concluded that, pure and  $\text{Cu}^{2+}$  doped CdO mediated degradation of methylene blue promises to be a versatile, economic, environmentally benign and efficient method of waste water treatment, if all parameters are properly optimized. In the Raman spectra, shift has been observed in the prominent peak positions of the doped samples due to the effect of additive ions.

## References

- [1] Z. Zhao, D. L. Morel, C. S. Ferekides, Thin Solid Films 413 (2002) 203.
- [2] M. Yan, M. Lane, C. R. Kannewurf, R. P. H. Chang, Appl. Phys. Lett. 78 (2001) 02342.
- [3] B. Sahin, Y. Gulen, F. Bayansal, H. A. Cetinkara, H. S. Guder, Superlattices Microstruct. 65 (2014) 56–63.
- [4] D. M. Carballeda-Galicia, R. Castanedo-Perez, O. Jimenez-Sandoval, S. Jimenez-Sandoval, G. Torres-Delgado, C. I. Zuniga-Romero, Thin Solid Films 371 (2000) 105.
- [5] Z. Zhao, D. L. Morel, C. S. Ferekides, 2002. Thin Solid Films 413, 203.
- [6] A. J. Freeman, K. R. Poeppelmeier, T. O. Mason, R. P. H. Chang, T. J. Marks, 2000. Mater. Res. Soc. Bull. 25, 45.
- [7] R. Maity, K. K. Chattopadhyay, 2006. Sol. Energy Mater. Sol. Cells 90, 597.
- [8] S. Shu, Y. Yang, J. E. Medvedova, J. R. Ireland, A. W. Metz, J. Ni, C. R. Kannewurf, A. J. Freeman, T. J. Tobin, 2004. J. Am. Chem. Soc. 126, 13787.
- [9] Yang, Yu., S. J. Shu, J. E. Medvedeva, J. R. Ireland, A. W. Metz, Jun, Ni, M. C. Hersam, A. J. Freeman, T. J. Marks, 2005. J. Am. Chem. Soc. 127, 8796.
- [10] G. Singh, I.P.S. Kapoor, R. Dubey, P. Srivastava, Mater. Sci. Eng. B 176 (2011) 121.
- [11] A.S. Kamble, R.C. Pawar, N.L. Tarwal, L.D. More, P.S. Patil, Mater. Lett. 65 (2011) 488.
- [12] J. B. Raoof, Ojani, and A. Kiani, J. Electroanal. Chem. 515 (2000) 45.
- [13] Li Hui, Zhang Yongzhe, Pan Xiaojun, Zhang Hongliang, Wang Tao, Xie Erqing, Journal of Nanoparticle Research 11 (2009) 917–921
- [14] M. Vigneshwaran, R. Chandiramouli, B.G. Jeyaprakash, D. Balamurugan, J. Appl. Sci. 12 (2012) 1754.
- [15] V. Ramasam, K. Praba, G. Murugadoss, Spectrochim. Acta, Part A 96 (2012) 963.
- [16] K. Gurumurugan, D. Mangalaraj, S.K. Narayandass, J. Electron. Matter. 25 (1996) 765.
- [17] M. Ristic, S. Popovic, S. Music, Mater. Lett. 58 (2004) 2494.
- [18] R. Cusco, J. Ibanez, N. D. Amador, L. Artus, J. Z. Perez, and V. M. Sanjose, J. Appl. Phys. 107, 063519 (2010).
- [19] R. Oliva, J. Ibanez, L. Artus, R. Cusco, J. Zuniga-Perez, and V. Munoz-Sanjose, J. Appl. Phys. 113, 053514 (2013).

- [20] J. W. Robinson 1991 Practical handbook of spectroscopy (ed.) J W Robinson (USA: CRC Press Inc.) 1st ed., Ch. 5, p. 533
- [21] G. Gouadec, P. Colomban, Prog. Cryst. Growth Charact. Mater. 53 (2007) 1.
- [22] F. Wang, D. Zhao, Z. Guo, L. Liu, Z. Zhang, D. Shen, Nanoscale 5 (2013) 2864–2869.
- [23] Y. Zheng, C. Chen, Y. Zhan, X. Lin, Q. Zheng, K. Wei, J. Zhu, Journal of Physical Chemistry C 112 (2008) 10773–10777.
- [24] A. I. Inamdar, A. C. Sonavanl, S. K. Sharma, H. Im, P. S. Patil, J. Alloys Compd 495 (2010) 76.
- [25] Alamgir, WasiKhan, Shabbir Ahmad, A. H. Naqvi, Mater. Lett. 133 (2014) 28.
- [26] L. Wang, L. Chang, B. Zhao, Z. Yuan, G. Shao, and W. Zheng, Inorg. Chem. 47 (2008) 1443.